Applied Surface Science Advances 34 (2026) 101051

Contents lists available at ScienceDirect

Applied Surface Science Advances

journal homepage: www.sciencedirect.com/journal/applied-surface-science-advances

Full Length Article

Surface DBD plasma functionalization of the interior of PVC and PTFE tubes: effects on surface properties and environmental safety assessment of leaching

Oleksandr Galmiz [a,b,*], Giulia Tomei [c], Ester Marotta [c], Zdenko Machala [a]

[a] Division of Environmental Physics, Faculty of Mathematics, Physics and Informatics, Comenius University in Bratislava, Mlynská dolina, 842 48, Bratislava, Slovakia
[b] CEPLANT, Department of Plasma Physics and Technology, Faculty of Science, Masaryk University, Kotlárská 2, 61137, Brno, Czech Republic
[c] Department of Chemical Sciences, University of Padova, Via Marzolo 1, 35131, Padova, Italy

ARTICLE INFO

Keywords:
Surface DBD
Non-thermal plasma
Polymer tubes
Degradation
Leaching
PFAS release

ABSTRACT

This study investigates the internal surface modification of polytetrafluoroethylene (PTFE) and poly(vinyl chloride) (PVC) tubes using a liquid-electrode surface dielectric barrier discharge (SDBD) plasma system. The approach addresses the "hollow body problem" by enabling uniform treatment of narrow internal geometries without vacuum conditions, while maintaining temperatures below the thermal deformation limits of the polymers. Water contact angle measurements showed successful conversion from hydrophobic to wettable surfaces (WCA ≈ 65–75°) with stable properties over 25 days, while X-ray photoelectron spectroscopy confirmed significant surface chemical restructuring, including approximately 50% fluorine replacement in PTFE. Furthermore, High-Performance Liquid Chromatography coupled with Mass Spectrometry (HPLC/MS) enabled an integrated environmental safety assessment. The analysis revealed trace perfluorocarboxylic acids (C3–C8) originating from PTFE as process-related byproducts that remained non-leachable after treatment. For PVC, the study differentiated between temperature-induced diffusion of bis(2-ethylhexyl) phthalate (DEHP) and the formation of phthalic acid as an indicator of plasma-induced oxidative degradation. Ultimately, these results demonstrate that SDBD plasma treatment is an effective method for modifying polymer tube surfaces while preserving material integrity and limiting hazardous substance release, providing critical insights into the environmental and biomedical safety of polymer plasma treatment systems to support their potential use in medical and related applications.

1. Introduction

Non-thermal atmospheric pressure plasmas have been extensively investigated for a wide range of applications, including ozone generation, pollution control, and plasma medicine [1–4]. Among these applications, plasma-based surface modification of polymers has emerged as a particularly impactful area. In such processes, active plasma components (including ions, excited species, radiation, and radicals) interact with material surfaces, leading to contaminant removal and the incorporation of functional groups. As a result, key surface properties such as wettability, adhesion, and printability can be significantly enhanced [5–8].

While planar surface modification is well-understood, the "hollow body problem", achieving uniform internal treatment of hollow objects like tubes or catheters, remains a challenge, because plasma cannot penetrate the tube to achieve a homogeneous modification of the inner surface. Although several methods have been proposed to generate plasma inside tubes under atmospheric and low-pressure conditions [9–15], only a limited number of these approaches are suitable for the treatment of tubes with lengths on the order of meters.

To address this limitation, our research group previously developed an innovative plasma reactor based on a surface dielectric barrier discharge (SDBD) that utilizes aqueous solutions as discharge electrodes. In this configuration, the plasma is ignited at the "three-phase point" between the ambient air, the liquid meniscus, and the dielectric polymer wall. This method allows modification of inner and/or outer tube

* Corresponding author at: Division of Environmental Physics, Faculty of Mathematics, Physics and Informatics, Comenius University in Bratislava, Mlynská dolina, 842 48, Bratislava, Slovakia.
E-mail address: oleksandr.galmiz@uniba.sk (O. Galmiz).

https://doi.org/10.1016/j.apsadv.2026.101051
Received 30 April 2026; Received in revised form 20 August 2026; Accepted 21 August 2026

surfaces by moving a "plasma ring" along the tube geometry [16–18]. The integration of an aqueous phase into the plasma discharge architecture provides critical operational benefits: it facilitates surface temperature control, minimizes thermal damage to polymers with low glass transition temperatures (T_g), and enables in-situ cleaning by removing loosely bound low molecular weight oxidized material (LMWOM) [16,19,20]. Also, plasma interactions with liquids generate highly reactive species such as hydroxyl radicals (•OH), atomic oxygen (O), and hydrogen peroxide (H_2O_2) [4,18,21,22].

This study evaluates the performance of the liquid-electrode SDBD system on two distinct tubular polymer substrates: non-polar polytetrafluoroethylene (PTFE) and polar plasticized poly(vinyl chloride) (PVC). Although plasma effectively modifies PTFE via defluorination and the introduction of polar groups [23,24], the potential release of regulated per- and polyfluoroalkyl substances (PFAS) during treatment remains insufficiently investigated, representing a critical environmental and health concern [25–27]. Similarly, while PVC is widely used in medical applications, its flexibility relies on migrating plasticizers like bis(2-ethylhexyl) phthalate (DEHP) [28–30], and the impact of plasma treatment on plasticizer leaching is poorly understood [31–33]. Despite the growing adoption of plasma methods, a major research gap remains in the simultaneous material functionalization and potential chemical leaching of treated polymers.

To bridge this gap, this work systematically investigates SDBD plasma treatment on PTFE and PVC tubes, utilizing advanced diagnostics, including Water Contact Angle (WCA) measurement, Scanning Electron Microscopy (SEM), Confocal Laser Microscopy (CLM), and X-ray Photoelectron Spectroscopy (XPS), to correlate discharge physics with interfacial chemical and morphological evolution. Crucially, High-Performance Liquid Chromatography coupled with Mass Spectrometry (HPLC/MS) is employed to monitor the process and leaching of trace concentrations of PFAS and DEHP byproducts. To the best of our knowledge, this research represents the first integrated assessment that simultaneously addresses surface functionalization efficiency and safety considerations. The findings contribute to establishing a foundation for the safe implementation of plasma technologies in industrial applications, particularly in sectors with stringent regulatory requirements, such as the medical and food industries.

2. Experimental setup

2.1. Materials

Two types of tubes were examined. The PVC tube, sourced from GUMEX, s.r.o (Czech Republic), had an outer diameter of 9 mm and an inner diameter of 6.5 mm. The PTFE tube, obtained from Goodfellow Company (UK), had outer and inner diameters of 9.25 mm and 8.5 mm, respectively.

The following chemicals: Bis(2-ethylhexyl) phthalate (DEHP, PESTANAL®, analytical standard), phthalic acid (puriss. p.a., ≥99.5%), oxalic acid (p.a. grade), perfluorooctanoic acid (PFOA, purity ≥ 96%), perfluoroheptanoic acid (PFHpA, purity 99%), perfluorohexanoic acid (PFHxA, purity ≥ 98%), perfluoropentanoic acid (PFPA, purity ≥ 98%), and perfluorobutanoic acid (PFBA, purity ≥ 98%), methanol (HPLC PLUS grade 99.9%), formic acid (puriss. p.a., ACS reagent, ≥98%), ammonium acetate (reagent grade purity ≥ 98%), were purchased from Merck.

Oxalic acid (Sigma-Aldrich, p.a. grade) was diluted in distilled water to enhance the conductivity of water-based electrodes.

2.2. SDBD plasma treatment set-up

Fig. 1 presents a schematic of the assembly and images of the generated electrical-discharge plasma. To facilitate handling, the tubes were cut into lengths of 13–15 cm. The total length of the tube actively treated during the experiments was 10 cm. However, it should be mentioned that the proposed treatment principle is not inherently limited to this length. The process can be extended to longer tubes by appropriate modifications of the reactor configuration, while maintaining the same treatment concept.

The experimental setup consisted of a glass vessel (300 mL) containing an oxalic acid solution in distilled water, into which the empty polymer tube sealed at the bottom was immersed (Fig. 1). Subsequently, the tube was gradually filled with the same solution using a pump. The controlled filling process caused the gas–liquid interface inside the tube to move upward, resulting in the upward propagation of the plasma ring along the inner tube wall. Since the discharge is generated at the three-phase contact point between the gas phase, liquid phase, and polymer surface, the movement of this interface enables sequential exposure and modification of the entire internal surface area. The liquid was pumped into the tube at varying flow rates, corresponding to the treatment times of 1.5–8 s. Due to the limited volume of the PVC tubes, the treatment time of these tubes was kept the same (8 s). The only variable parameter was the discharge power. To ensure electrical contact with the inner liquid volume, a stainless-steel wire was inserted into the tube. To suppress undesired volume discharge and to prevent plasma distortion caused by falling water, an additional dielectric tube surrounding this wire was employed as a shielding element.

The power for the electrodes was supplied by a high-voltage resonance generator (Lifetech, 300 W). To regulate the frequency of the HV generator pulses, we employed the function generator GW-Instek SFG-2104. The frequency of these pulses was fine-tuned between 30 and 37

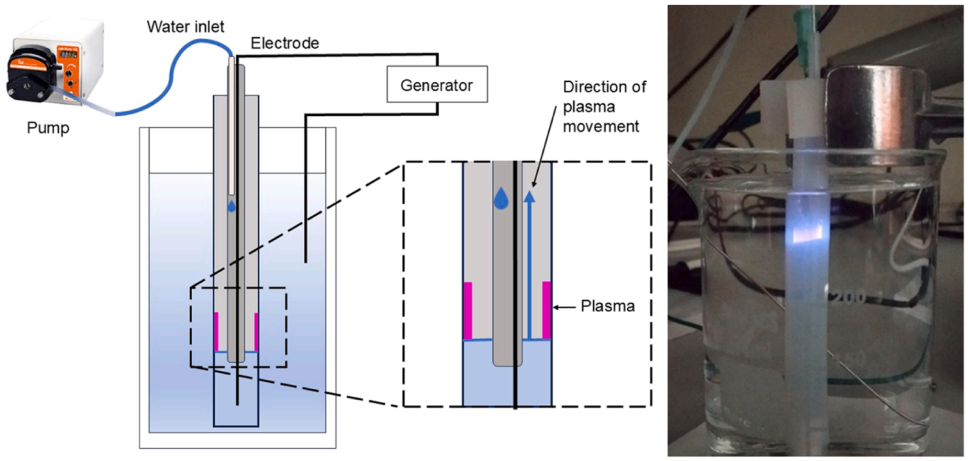

Fig. 1. Schematic setup and photo of the SDBD configuration for the inner side tube treatment.

kHz to achieve optimal resonance conditions, which varied as the tube was filled with liquid.

To monitor the electrical characteristics of the discharge, we used a digital oscilloscope (Tektronix TBS 2104, 100 MHz, 1 GSa/s) connected to both a high-voltage (Tektronix P6015A) and a current (Pearson Electronics 2877) probe. The discharge power, controlled via a laboratory power source, was measured using the Lissajous figure method. The additional capacitor (10 nF) was added to the circuit to perform these measurements. Throughout our experiments, the system operated at applied power levels up to 15 W, with the discharge plasma igniting along the inner perimeter of the tube. The maximum voltage applied under the experimental conditions of this study was approximately 11 and 13 kV peak-to-peak, corresponding to discharge powers of 7 and 15 W, respectively. The standard deviation of the measured power was estimated to be at most 0.5 W.

Because the liquid level inside the tube changes during treatment, the electrical characteristics of the discharge may vary slightly with the position of the gas–liquid interface. Therefore, before the experiments, the discharge power was determined at different liquid levels.

To unify the results obtained throughout this study, only the plasma treatment parameters for which the leaching tests were performed will be shown here.

2.3. Sample preparation and HPLC/MS measurements

Prior to treatment, the tubes were rinsed with distilled water to remove any potential surface contaminants. Subsequently, they were allowed to air-dry under laboratory conditions. After the treatment, a liquid sample designated T0 was collected from the inner volume of the tube. The tubes were washed with distilled water and then filled with 5.6 mL of 0.9% NaCl solution for PTFE and 3 mL for PVC. The PTFE samples were bent into a V shape, and the PVC samples were bent into a U shape and sealed at both ends with PARAFILM. Both types of samples were immersed in glass beakers filled with distilled water. These beakers were heated and maintained at 37 °C. For the leaching test, the liquid samples were collected at 4, 24, 48, 72, and 96 h. Specifically, 500 μL of solution was collected from inside the PTFE tube and 200 μL from inside the PVC tube.

HPLC/MS analyses of the treatment liquid (T0) and leaching solutions were performed using an Agilent 1200 series HPLC coupled to a Thermo Scientific LTQ XL mass spectrometer equipped with an electrospray source and a linear ion trap analyzer. The chromatographic column was an InfinityLab Poroshell 120 EC—C18, 2.1 × 100 mm, 2.7 μm (Agilent Technologies).

2.3.1. Analysis of PVC leaching

The eluents used for chromatographic separation of PVC leaching solutions are Milli-Q water + 0.1% formic acid (A) and methanol + 0.1% formic acid (B). The gradient for eluent B was as follows: 10% for 2 min, from 10% to 100% in 23 min, 100% for 5 min. The flow rate was set at 0.3 mL/min, and the injection volume was 20 μL. Samples ionization was performed both in positive and negative mode (ESI+/−), with a spray of 3 kV and a source temperature of 300 °C. Optimized values for the gas flows were as follows: Sheath gas = 35 a.u., Auxiliary gas = 10 a.u., Sweep gas = 0 a.u. The acquisition was performed in a full scan.

DEHP was quantified in positive ion mode ($[M + H]^+$, *m/z* 391, retention time (RT) = 29.86 min) using a calibration curve with dimethyl phthalate (DMP, *m/z* 195, RT = 17.75 min) as the internal standard. The limit of detection for DEHP was $2{\cdot}10^{-7}$ M.

Phthalic acid was quantified in negative ion mode ($[M - H]^-$, *m/z* 165, RT = 12.23 min) using a calibration curve, with disodium terephthalate (*m/z* 165, RT = 13.89 min) as the internal standard. The limit of detection for phthalic acid was $2{\cdot}10^{-7}$ M.

2.3.2. Analysis of PFAS released in and after PTFE plasma treatment

The eluents used for chromatographic separation of the PTFE leaching solutions are 5 mM ammonium acetate in Milli-Q water (A) and methanol (B). The gradient for eluent B was as follows: from 10% to 100% in 22 min, then held at 100% for 4 min. The flow rate was set at 0.3 mL/min, and the injection volume was 10 μL. Sample ionization was performed in negative ion mode (ESI−), with a spray voltage of 2.5 kV and a source temperature of 300 °C. Optimized values for the gas flows were as follows: Sheath gas = 35 a.u., Auxiliary gas = 10 a.u., Sweep gas = 0 a.u.

The acquisition was performed in full-scan (FS) mode, and deprotonated ions $[M - H]^-$were detected. The quantification of perfluorononanoic acid (PFNA, *m/z* 463), perfluorooctanoic acid (PFOA, *m/z* 413), perfluoroheptanoic acid (PFHpA, *m/z* 363), perfluorohexanoic acid (PFHxA, *m/z* 313), perfluoropentanoic acid (PFPeA, *m/z* 263), perfluorobutanoic acid (PFBA, *m/z* 213) and perfluoropropanoic acid (PFPrA, *m/z* 163) was based on internal calibration curves, using perfluorooctanesulfonic acid (PFOS, *m/z* 499) as the internal standard. The limit of detection was $5{\cdot}10^{-9}$ M for PFNA and PFOA, $1{\cdot}10^{-8}$ M for PFHpA, PFHxA and PFPeA, $3{\cdot}10^{-8}$ M for PFBA and PFPrA.

2.4. Surface morphology and roughness measurements

Static contact angle measurements were performed on the reference and plasma-treated inner surfaces of tubes (using a KRUSS DSA30) with surface curvature corrections applied. The water contact angle (WCA) was determined by the sessile drop technique (1 μL volume). Deionized water was selected as the test liquid.

The surface morphology was studied using a scanning electron microscope (MIRA3; TESCAN, Brno, Czech Republic). To achieve better visualization and prevent charging, the samples were covered by a 10 nm Au-Pd composite layer. All sample surfaces were scanned using a secondary electron emission detector at an acceleration voltage of 10 kV, in the depth regime, with a working distance of 9 mm.

The surface roughness of the samples was investigated with an Olympus LEXT OLS4000 confocal microscope equipped with a 405 nm semiconductor laser. Pictures were analyzed by Mountain-sMap™ Premium v6.2 software. The optimal area for determining surface roughness was 646 × 646 μm^2. The arithmetical mean height (Ra) and areal average roughness (Sa) were used as the parameters describing surface roughness. A line profile was measured on the surface that possessed minimal reliefs due to the manufacturing method.

2.5. X-ray photoelectron spectroscopy

To characterize the elemental surface composition of the polymer surfaces before and after plasma treatment, X-ray photoelectron spectroscopy using an ESCALAB 250Xi (Thermo Fischer Scientific) has been employed. An X-ray beam with a power of 200 W (650 μm^2 spot size) was used. The pass energies were set to 50 and 20 eV for wide-scan and high-resolution elemental scans, respectively. These pass energies correspond to energy resolutions of 1.0 and 0.1 eV, respectively. An electron flood gun was used to compensate for surface charge.

Spectra were referenced to the hydrocarbon type C 1 s component set at a binding energy of 285 eV. Spectra calibration, processing, and fitting routines were done using Avantage software.

3. Results and discussion

3.1. Characterization of the SDBD plasma

The stability and homogeneity of atmospheric-pressure discharges are fundamental to achieving uniform material modification. In our SDBD configuration, the liquid electrode serves a dual role: it provides the high-voltage potential required for gas breakdown and acts as a resistive stabilizer that prevents microdischarges from transitioning into destructive thermal arcs. While any electrically conductive liquid can

technically serve as an electrode, low-conductivity solutions tend to heat up when used as electrodes. To mitigate this issue while maintaining the conductivity of the water-based electrode high, we used a solution of oxalic acid in distilled water, resulting in a conductivity of 8 mS cm^{-1}.

The plasma generated in this study exhibits a filamentary nature, characterized by transient microdischarges propagating along the inner polymer surface. High-speed imaging has previously revealed that such discharges consist of numerous short-lived (< 10 ns) microdischarges [18]. However, due to the airflow induced by the discharge itself [34], combined with the rapid movement and high repetition frequency (30–37 kHz) of these microdischarges, the plasma visually appears diffuse and quasi-homogeneous.

This optical homogeneity, despite the underlying filamentary discharge structure, is advantageous for polymer surface treatment, as it ensures macroscopically uniform exposure of the material while leveraging the localized energy delivery of microdischarges.

Visual monitoring indicated that as the discharge power increased from 2 W to 7 W, the area covered by the plasma ring expanded and the filament density increased, resulting in a more intense yet stable treatment environment. At the lower discharge power, the plasma filaments reached a length of 2 mm, whereas at 7 W, their length increased to 4 mm.

Fig. 2 shows a typical pattern for DBD operations in ambient air. The measured current has two components. The first is a sinusoidal displacement current flowing through the electrode capacitance. The second component consists of a series of narrow pulses that appear in each half-cycle of the applied voltage, starting at the onset value and ending at the peak voltage value. They correspond to the DBD microdischarges. To demonstrate the electrical characteristics of the SDBD with liquid electrodes, the voltage and current waveforms at an elevated applied power of 25 W are presented. This condition was selected exclusively for illustrative purposes, as the higher discharge power produces more pronounced conduction current peaks, enabling clearer separation of the plasma-related current contribution from the capacitive displacement current. Although the material treatments in this study were performed at lower powers of 2 W and 7 W, these conditions correspond to the same SDBD operating regime. The reduction in applied power primarily decreases the magnitude and occurrence frequency of individual microdischarges, while preserving the characteristic asymmetric voltage–current behaviour of the discharge. Therefore, the waveform shown in Fig. 2b is representative of the fundamental electrical behaviour of the SDBD system and is not intended to represent the exact electrical conditions applied during polymer treatment.

Electrical measurements revealed a distinct asymmetry between the positive and negative half-cycles of the applied voltage. Specifically, the positive-polarity half-cycle exhibited a significantly higher current-pulse amplitude than the negative half-cycle. This finding is consistent with previously reported electrical characteristics of SDBDs in actuator configurations [35] and similar plasma systems [17,36–38]. The enhanced current amplitude during the positive half-cycle likely results from asymmetrical charge accumulation on the polymer or dielectric surface, influencing the initiation and propagation of the discharge filaments.

The discharge asymmetry, together with the inherently filamentary nature of the plasma, has direct implications for polymer surface modification. Although the plasma may appear visually macroscopically diffuse, the filaments are in fact highly microscopically localized. Extremely high electric fields initiate the discharge at the three-phase contact point, which forms at the interface between air, the liquid surface, and the polymer tube wall [39]. This leads to the formation of transient microdischarges that create spatially confined regions with elevated energy density and high concentrations of reactive species. These localized regions are responsible for initiating chemical modifications at the polymer interface, such as bond scission, oxidation, and crosslinking. However, a typical single microdischarge duration is as short as 10–100 ns [40] [find reference!], way too short to allow for energy transfer able to cause microscopic local thermal damage to the polymer material.

To additionally confirm that these material modifications are not primarily caused by thermal effects, the non-thermal character of the discharge was evaluated using time-integrated optical emission spectroscopy (OES) in our previous studies [38,40,41]. The recorded spectra showed the presence of the second positive system of molecular nitrogen (N_2 $C^3\Pi_u \rightarrow B^3\Pi g$), the first negative system of nitrogen ions (N_2^+ $B^2\Sigma_u^+ \rightarrow X^2\Sigma g^+$), and OH ($A^2\Sigma^+ \rightarrow X^2\Pi$) emission bands. Analysis of the rotational structure of the N_2 second positive system indicated a rotational (i.e., gas) temperature of approximately 300–350 K at a discharge power of 15 W, demonstrating that the plasma operates close to ambient temperature. This temperature is substantially below the thermal deformation thresholds of both PTFE and PVC, indicating that the observed surface modifications are not driven by macroscopic thermal effects but predominantly by plasma-induced chemical interactions involving reactive oxygen and nitrogen species. Although localized transient heating within individual microdischarge channels cannot be completely excluded, such effects are limited to the near-surface region and may only assist secondary processes, such as the diffusion of low-molecular-weight species in plasticized PVC, rather than causing bulk thermal degradation. Therefore, optimization of plasma parameters, including polarity, frequency, and gas composition, remains essential for controlling the balance between treatment uniformity and sufficient reactive species generation for effective surface functionalization. A detailed electrical and optical characterization of the

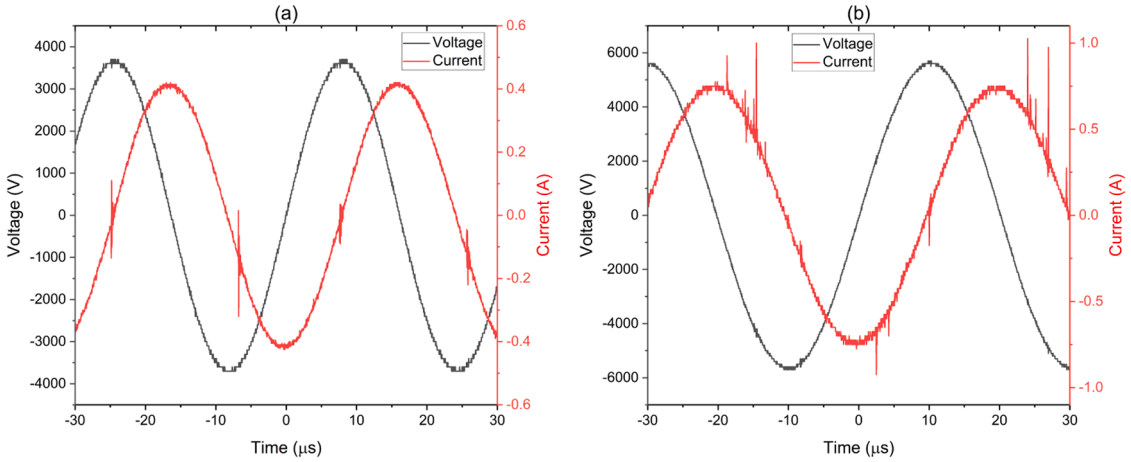

Fig. 2. Typical voltage and current waveforms of the SDBD with liquid electrodes corresponding to the discharge power 7 W (a) and 25 W (b).

discharge, including OES, ICCD imaging, and electrical measurements, has been reported in our previous studies [18,38,41,42].

3.2. Water contact angle measurements

WCA measurements were performed during this study as a rapid indicator of plasma treatment-induced hydrophilization. The reported contact angle values represent a statistical evaluation of the overall surface wettability rather than a local measurement at an individual plasma-affected spot. The relatively narrow range of measured WCA values and their reproducibility indicate that the treatment effect is distributed across the processed area. The reduction in WCA represents an increase in the surface free energy of the polymer, thereby facilitating better interaction with biological fluids and coatings. Surface curvature corrections were applied to precisely determine the water contact angle on the inner surface of the tube. As shown in Fig. 3, the WCA of the reference material was approximately 95° for PTFE and approximately 105° for PVC. These values are usual for such materials. This indicates that the material surface chemical composition is hydrophobic and does not contain polar elements. After the plasma treatment, the WCA decreased to 55–60° for both materials, indicating hydrophilization.

The effects obtained on WCA in this study are weaker in comparison to the results with the same materials obtained in our previous studies [16,43]. These differences could be explained by the much lower treatment time and discharge powers used in this study. By increasing the liquid flow, thus shortening the treatment time, we tried to increase the speed of the polymer tube plasma treatment.

A significant decrease in water contact angle was also observed in the literature after a DBD plasma treatment. The contact angle of the processed PTFE decreased with increased plasma power, treatment cycle, and electrode gap within the range of investigation. It was observed that the higher the power of plasma treatment, the greater the resultant induced surface oxygen concentration. The authors stated that the contact angle of PTFE is closely linked to the surface oxygen (hydroxyl) concentration [44]. The results obtained in the present study are close to the results presented by Fang et al. [45] where a DBD plasma treatment of PTFE was studied. The static contact angle decreased from 118 ° for the reference samples to a minimum of 70 ° after a 40-second DBD treatment. Compared with that study, the shorter treatment time in our case offers a significant advantage.

Similarly, results on the dependence of the PVC water contact angle on different plasma treatments have been reported in [46]. It has been shown that different plasma modifications have different effects on the hydrophilicity of PVC films, and the polymer wettability depends on the presence of polar groups on the surface. Our treatment of the PVC material did not result in a similarly drastic decrease in WCA. However, it is important to emphasize that, as observed in the case of PTFE treatment, the plasma exposure times reported in these studies were substantially longer than those applied in the present work.

It is well established that plasma-treated polymers are prone to an aging phenomenon referred to as hydrophobic recovery. This effect is primarily driven by the inward reorientation of newly introduced polar groups from the surface toward the polymer bulk [47,48]. In the present case, however, the surface remained hydrophilic even after 25 days, suggesting the formation of a new, relatively stable layer of highly cross-linked polymer and/or chemically modified plasticizers. A comparable behavior was observed by Morent et al. [49], who examined the post-treatment aging of PP and PET films exposed to plasmas generated in air, helium, and argon. Their results demonstrated that extensive cross-linking reduces chain mobility at the surface and consequently suppresses hydrophobic recovery.

The results obtained are significant for potential manufacturers, as they should ensure that materials treated with SDBD retain their functional properties throughout the supply chain and storage cycle.

3.3. Topographical evolution and roughness dynamics

3.3.1. Scanning electron microscopy analysis

The surface morphology of PTFE and PVC tubes was examined before and after plasma treatment using scanning electron microscopy. The plasma treatment exposure was 8 s, and the plasma power was 7 W for each sample presented in Fig. 4. The surface of the reference PTFE tube shows some scratches of different depths chaotically located on the surface, with the deepest scratches alongside the tube. This defect of the material probably occurred during the manufacturing procedure. The PVC tube has a smoother surface with no significant scratches. The plasma treatment did not show any substantial modification in the morphology and the surface structure.

Despite the known etching effect of plasma on polymers, no significant morphological changes were observed in either material. This suggests that the combination of short treatment time (8 s) and low plasma power (7 W) effectively minimized the etching effects. Additionally, the propagation of plasma along the treated surface may have contributed to the preservation of the original surface structure.

3.3.2. Confocal laser microscopy

The surface morphology of PTFE and PVC tubes, both plasma treated and reference, was examined using confocal laser microscopy. This provided a more quantitative view of the topography through arithmetic mean height (R_a) and areal average roughness (S_a). The results are visualized in Fig. 5 and summarized in Tables 1 and 2.

Applying a discharge power of 2 W did not affect the surface of the PTFE tubes. A slight increase in the surface roughness (Ra) was observed when the plasma exposure time was increased to 8 s. The effect of plasma exposure time was more pronounced with a higher discharge power of 7 W. Both parameters, Sa and Ra, increased with exposure time

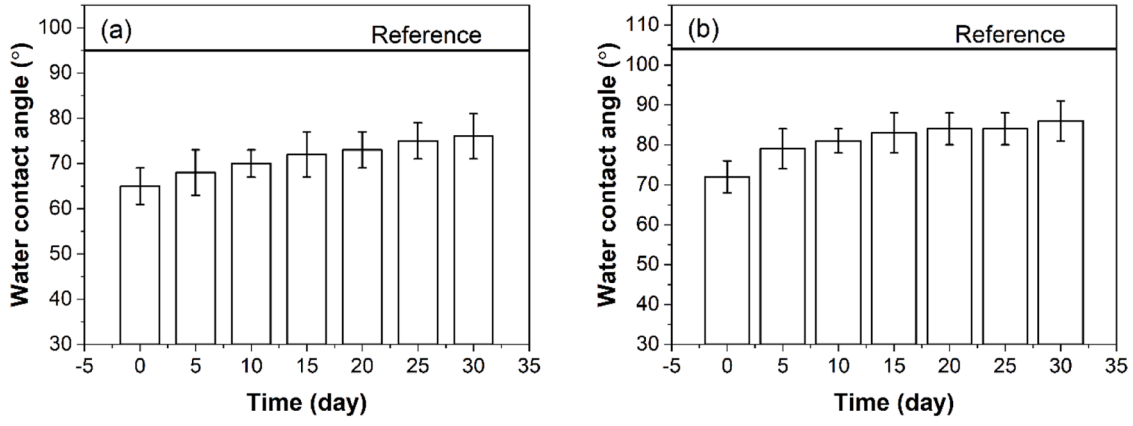

Fig. 3. Aging effect on plasma treated PTFE and PVC inner surfaces. The discharge power was 7 W, and the treatment time was 8 s.

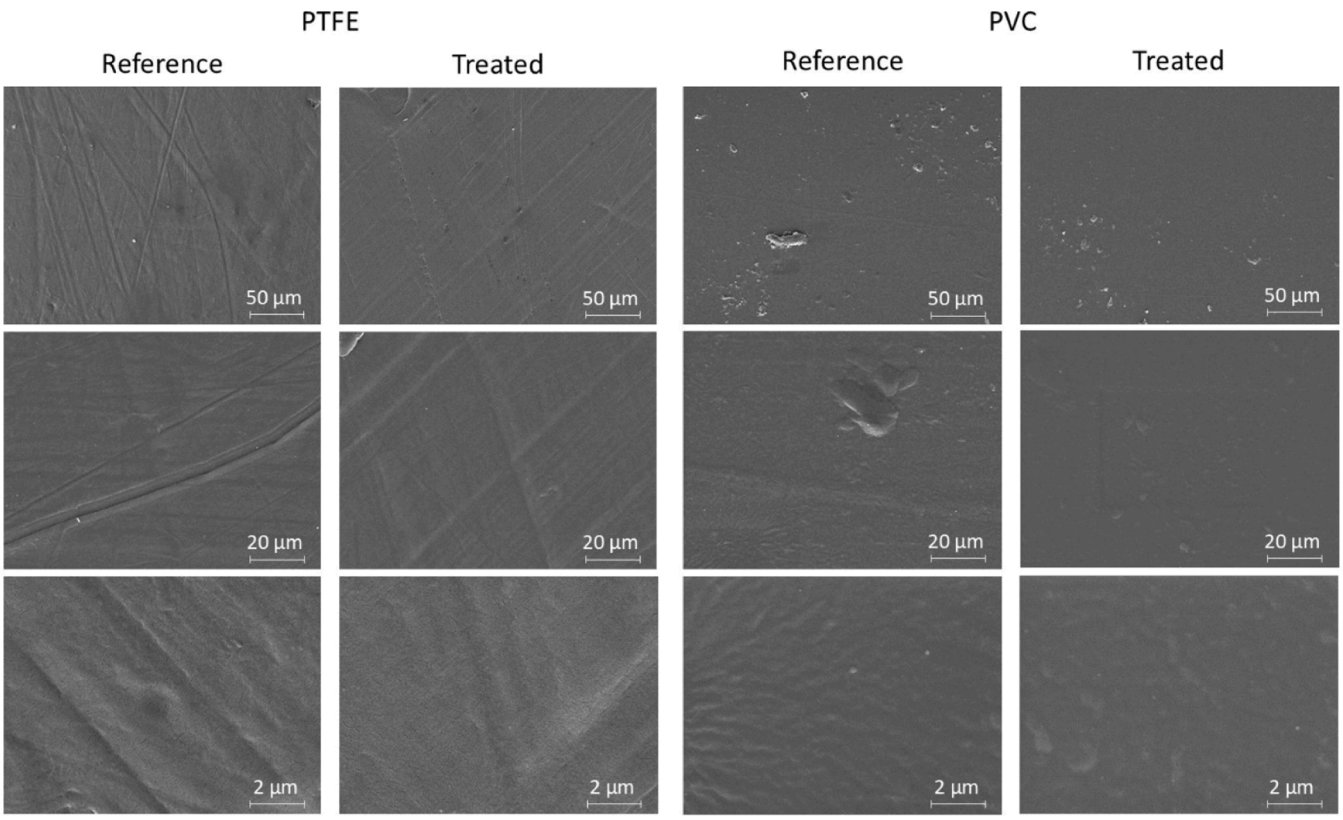

Fig. 4. SEM images of the reference and plasma treated inner surface of the PTFE and PVC tubes (discharge power 7 W, plasma exposure 8 s).

and exceeded the reference values, 205 and 118 nm for 4 s, and 219 and 124 nm for 8 s, respectively. Although high standard deviations, stemming from inherent manufacturing relief on the reference material, somewhat constrain the absolute statistical weight of these topographical shifts, this subtle response is primarily attributed to PTFE's robust semi-crystalline backbone and the exceptionally high bond energy of its carbon-fluorine (C-F) bonds, which confer high resistance to physical sputtering and extensive chemical etching [23,50].

In contrast, the plasma treatment caused a much more pronounced modification of the PVC surface. CLM image reveals that the reference PVC is quite uniform and has a smooth surface. The modification of the PVC surface with plasma treatments increased average surface roughness (Sa and Ra). It was clear that the reference PVC exhibits little surface roughness (Ra) and showed an average Ra of about 61 nm, while after the plasma treatment, Ra achieved 136 nm and 202 nm for discharge powers of 2 and 7 W, respectively. This increase aligns with previous literature indicating that high-power atmospheric DBD plasma leads to significant etching of PVC surfaces [51]. For instance, Bekkara et al. [52] reported that extended DBD treatment markedly modified PVC surface topography (increasing *S*a from 140 nm to 200 nm), with excessive treatment times ultimately causing material deformation and melting—a phenomenon similarly observed in our experiments when the plasma ring remained stationary [51]for at least 5 min.

The stark contrast in topographic outcomes between the two substrates highlights the distinct behavior of a semi-crystalline fluoropolymer versus an amorphous, plasticized polymer matrix. While PTFE's dense crystalline regions limit deep penetration and degradation by plasma species, the amorphous regions of PVC and the presence of mobile, unbonded plasticizer molecules (such as DEHP) create a more vulnerable matrix. Reactive plasma species interact much more intensely with the amorphous PVC structure, leading to preferential ablation and the generation of nanoscale "hillock-like" structures [53]. While this increased roughness can enhance the effective surface area for mechanical interlocking with adhesives or coatings, it represents a critical parameter that must be carefully balanced in medical catheter applications to prevent the mechanical anchorage of bacteria and subsequent biofilm formation.

3.4. X-ray photoelectron spectroscopy

3.4.1. PTFE samples

To detect the chemical changes on the surface of the treated material, XPS measurements were done. Samples of PTFE tubes were treated with two different powers and treatment times. The quantitative atomic percent concentration and ratios of reference and plasma-treated surfaces are presented in Table 3.

PTFE is primarily composed of carbon and fluorine, with a minor oxygen content (0.9%) attributed to the surface oxidation due to atmospheric exposure. The reference sample consists of about 35 at.% (atomic percentage) of carbon and 64 at.% of fluorine, which is close to the theoretical value.

Plasma treatments led to a decrease in fluorine content and a simultaneous increase in carbon and oxygen percentages. The reference PTFE surface exhibited an F/C ratio of 1.8. Following 8 s of treatment at 7 W, this ratio decreased to 0.68, representing a remarkable 50% replacement of surface fluorine with oxygen species. The decrease in F content may be caused by the plasma treatment (etching action) that removes the volatile fluorinated fragments from the PTFE [54].

The content of oxygen in the sample increased after treatment, and values in the range from 2% to 7.7% were achieved, depending on treatment conditions. This indicates the incorporation of oxygen into the polymer structure through surface oxidation during the plasma process. Following 8 s of treatment at 7 W, the O/C ratio increased by a factor of 4.6, from 0.03 to 0.14, while the atomic percentage of oxygen increased 8.5 times. As expected, longer treatment durations and higher discharge power led to greater oxygen incorporation, thus enhancing the surface

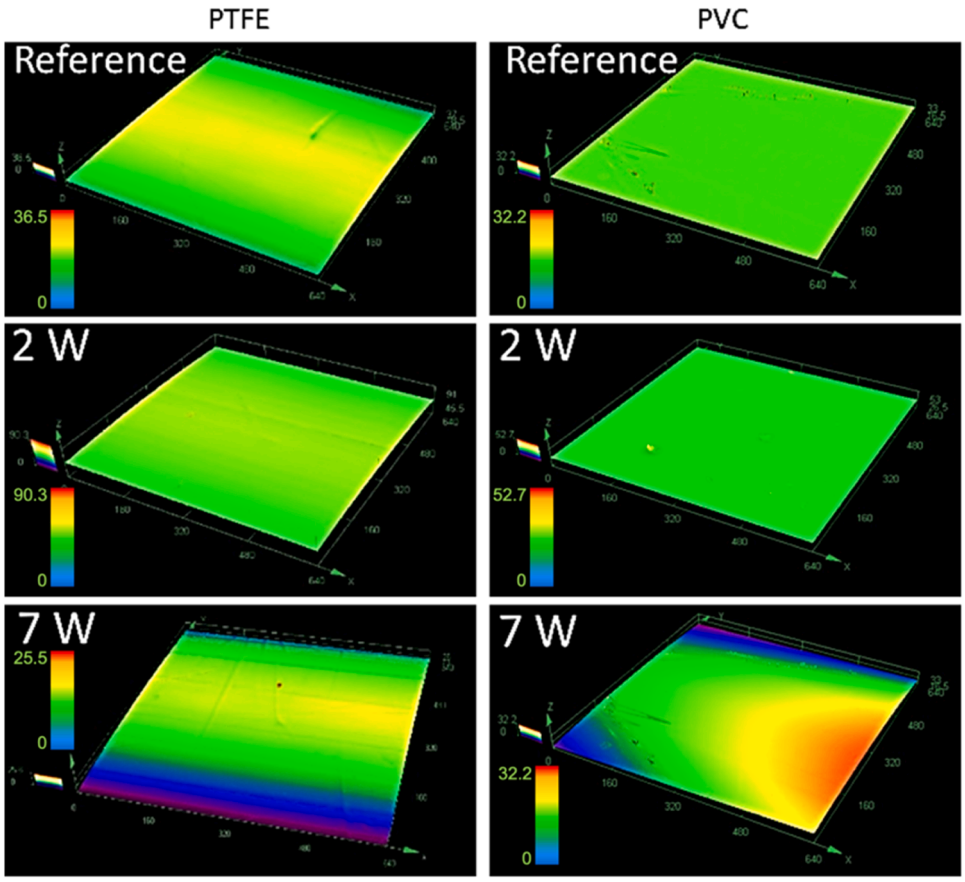

Fig. 5. Representative confocal laser microscopy surface topography maps of the reference and plasma-treated samples. Plasma exposure time: 8 s. Discharge powers are indicated in the photo. The colour scale represents the surface height and is shown individually for each image. Quantitative roughness parameters are summarized in Tables 1 and 2.

Table 1
Arithmetic mean surface roughness (Ra) and areal roughness (Sa) values of the PTFE tube surface.

Conditions	Sa [μm]	Ra [μm]
Reference	0.190 ± 0.024	0.086 ± 0.034
Plasma 2 W, 4 s	0.193 ± 0.084	0.087 ± 0.033
Plasma 2 W, 8 s	0.196 ± 0.026	0.098 ± 0.031
Plasma 7 W, 4 s	0.205 ± 0.029	0.118 ± 0.042
Plasma 7 W, 8 s	0.219 ± 0.034	0.124 ± 0.050

Table 2
Arithmetic mean surface roughness (Ra) and areal roughness (Sa) values of the PVC tube surface.

Conditions	Sa [μm]	Ra [μm]
Reference	0.086 ± 0.014	0.061 ± 0.014
Plasma 2 W, 8 s	0.137 ± 0.027	0.136 ± 0.034
Plasma 7 W, 8 s	0.186 ± 0.051	0.054

Table 3
Atomic percentage of elements on the surface of PTFE samples and F/C and O/C ratios obtained from XPS spectra.

Conditions	C	F	O	F/C	O/C
Reference	35.4	63.7	0.9	1.8	0.03
Plasma 2 W, 4 s	35.8	62.2	2	1.73	0.06
Plasma 2 W, 8 s	39.9	57.4	2.6	1.44	0.07
Plasma 7 W, 4 s	40.9	56.1	3	1.37	0.07
Plasma 7 W, 8 s	55.1	37.2	7.7	0.68	0.14

activation of the polymer.

To further understand the variety and content of oxygen-containing functional groups on modified PTFE surfaces, high-resolution XPS peak fitting was conducted. The high-resolution XPS analysis of the C 1 s and O 1 s spectra was performed and is presented in Fig. 6.

Deconvolution of the C 1 s spectrum using a Gaussian-Lorentzian method revealed the percentages of various chemical components (Table 4). The reference PTFE sample exhibited a C 1 s spectrum with two primary peaks: a hydrocarbon peak at 285.1 eV and a CF_2 peak at 292.4 eV. Following the treatments, the higher binding energy carbon contributions increase, and additionally, oxidized species emerge. Consequently, the C 1 s band now exhibits a long tail extending towards the high-energy side. The C 1 s envelope of the modified surfaces, as shown in Fig. 6, was fitted with five peaks, corresponding to binding energies of 285.1, 286.7, 288, 289.2, and 292.4 eV. These peaks are associated with C—C/C—H, C–O/C–OH, C═O/O–C–O, O–C═O/COOH, and CF_2/–CF–O– bonds, respectively.

The results in Fig. 6 and Table 4 indicate that plasma treatments lead to a reduction in the -CF_2- groups. Their initial percentage for the reference material is around 86.7%. After the plasma exposure, these values decreased to 28.9%, depending on the treatment conditions.

Treating the PTFE polymer also had a visible effect on the C–C (H) and other oxidized functional groups. Aliphatic carbon bonds C–C (285.0 eV) rose from 9.6% in the reference samples to 54.6% after the most intense treatment. Additionally, oxidized products such as aldehydes and ketones (C═O) increased. The O 1 s spectrum further confirmed the formation of COOH groups on the treated surface.

One of the primary effects of plasma treatment on PTFE is the introduction of polar functional groups onto the surface. The PTFE

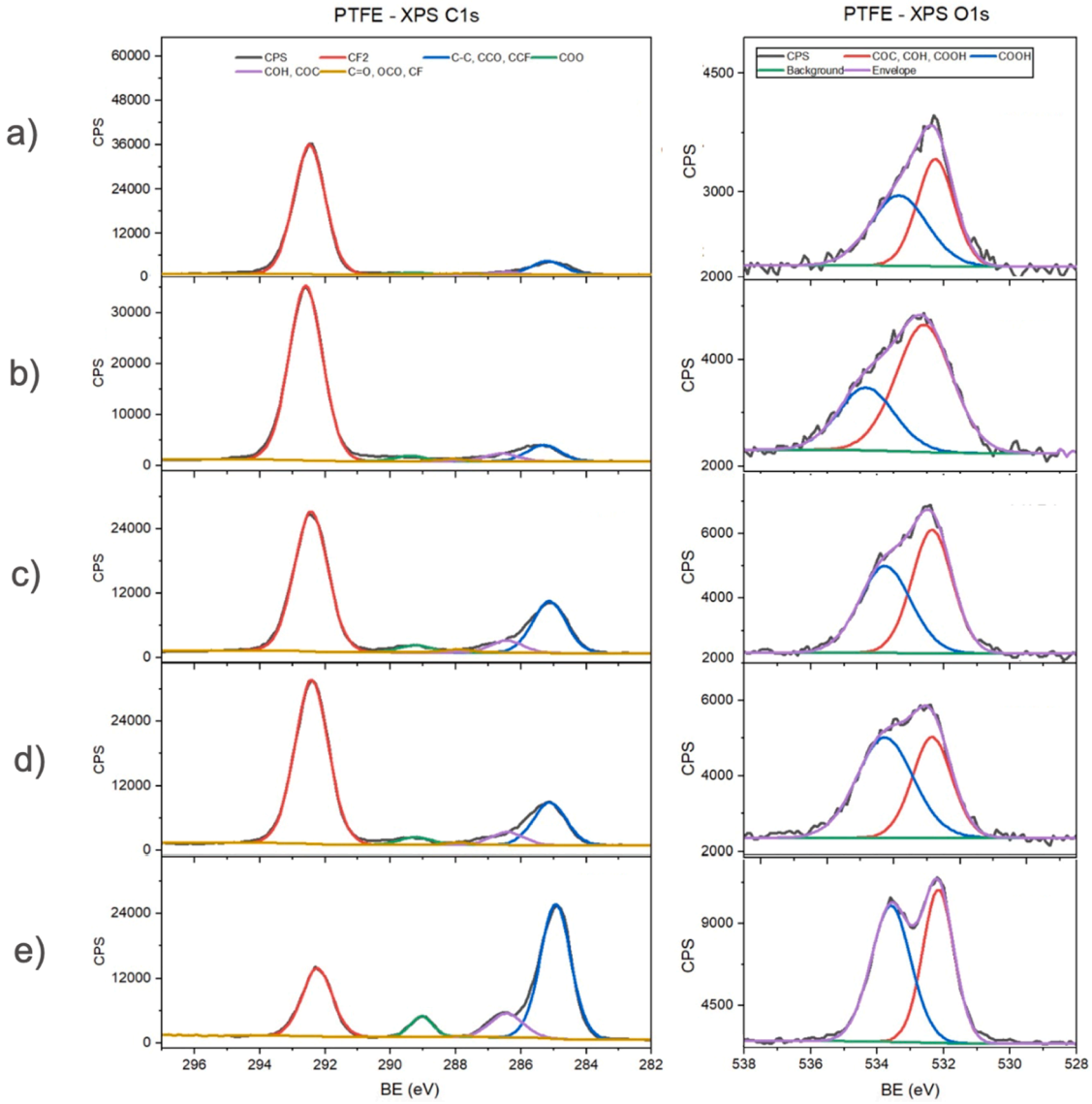

Fig. 6. XPS high-resolution C 1 s and O 1 s spectra of plasma treated PTFE tube surface: a) reference, b) discharge power 2 W, 4 s treatment, c) discharge power 2 W, 8 s treatment, d) discharge power 7 W, 4 s treatment, e) discharge power 7 W, 8 s treatment.

Table 4
The components of high-resolution C 1 s spectra and their percentage contributions.

Conditions	C-C/ C—H	C–O/ C–OH	C=O/ O–C–O	O–CO/ COOH	CF_2/ –CF–O–
BE, eV	285.1	286.7	288	289.2	292.4
Reference	9.6	1.6	0.6	1.5	86.7
Plasma 2 W, 4 s	7.8	3.9	1.0	2.8	84.4
Plasma 2 W, 8 s	21.2	5.4	1.2	3.1	69.1
Plasma 7 W, 4 s	18.3	6.7	0.9	3.7	70.5
Plasma 7 W, 8 s	54.6	10.3	0.2	6.1	28.9

polymer is composed of strong carbon-fluorine (C–F) bonds, which are among the most stable bonds in organic chemistry. However, the energy and reactivity of plasma species can oxidize some of these bonds, leading to defluorination and incorporation of oxygen-containing functional groups, like hydroxyl (–OH), carbonyl (C═O), and carboxyl (–COOH) groups.

The efficiency of the plasma surface treatment can be evaluated by the incorporation of oxygen and/or nitrogen onto the treated polymers. Similar to our results, Sarra-Bournet et al. [55] found a considerable amount of C–C component, which was explained by strong surface defluorination. Defluorination, resulting in a decreased F/C ratio, has also been observed by other researchers [56,57] during plasma treatment of PTFE.

Atmospheric air and liquid-film DBD plasma were used to improve the hydrophilicity of PTFE in [54], where the O content on the PTFE surface increased from 0.95% to 2.17% after air plasma modification, and liquid-film plasma modification further increased the O content to 2.47%. Wilson et al. [58] reported a defluorination process and introduction of unsaturated hydrocarbons and oxygen-containing moieties. However, storage in the air led to partial recovery towards the reference surface state, which was attributed to relaxation processes in the modified layer.

The effect of fluorine content decrease, accompanied by the oxygen content increase, was also observed by Fang et al. [45], where the oxygen content had a maximum value of 13% and 9% after 20 s of APGD and DBD treatment, respectively.

3.4.2. PVC samples

The reference PVC tube is composed primarily of carbon and oxygen, with minor amounts of chlorine and silicon. This composition was attributed to the presence of a significant amount of plasticizer (DEHP) and potential surface contaminants. Due to XPS's shallow analysis depth (approximately 3 nm), the PVC polymer itself may have been poorly detected. The elemental composition in at.% of reference and plasma-treated PVC samples is shown in Table 5.

Oxygen content on the surface increased after treatment by the SDBD plasma, influencing the O/C ratio, which changed from 0.12 to 0.16 and 0.22, applying 2 W and 7 W plasma power, respectively. This indicates surface grafting of reactive species during the treatment, as also reported by other researchers [59].

While PTFE samples underwent significant defluorination, leading to substantial changes in the spectral envelope, the surface modifications observed in PVC were less pronounced; therefore, the high-resolution XPS spectra of the C1s and O1s regions are not presented. The components of high-resolution C 1 s spectra and their percentage contributions are shown in Table 6.

The C—CHCl and C—Cl components are derived from the PVC polymer chain itself. Considering the chemical formula of the DEHP plasticizer, we can conclude that the O–C═O/COOH component originates from DEHP. The C—C/C—H component could originate from the polymer itself as well as from the DEHP. The C–O/C–OH and C═O/O–C–O components are new bonds that are formed by the plasma treatment.

Following the plasma treatment, there is a slight decrease in the C—C/C—H component, likely due to the oxidation of hydrocarbon groups, seen as an increase in the O–C═O/COOH, C–O/C–OH, and C═O/O–C–O components. This agrees with the increased hydrophilic effect discussed in the previous section.

A slight decrease in the C—CHCl component is observed and could be attributed to the degradation of the PVC polymeric backbone. Also, a slight increase of 2% in C—Cl bonds was detected.

One of the possible explanations could be the plasma etching of the upper layer of the tube, presumably composed mainly of DEHP plasticizer. This allows the signal corresponding to the PVC polymer to be detected during XPS analysis. These results contradict the findings of Balazs et al. [60], where a decrease in the C—CHCl peak was observed. However, the pristine PVC material is typically treated by plasma in the form of plates, which are much easier to handle. On the contrary, in our case, the PVC material is in the form of flexible tubes, which means that PVC has been stronger supplemented with plasticizers. This can be the reason why the elemental composition of the reference sample, as well as the effect of plasma treatment, differs.

Asadinezhad et al. used a Diffuse Coplanar SBD for altering the surface of PVC material. The reduction of WCA from 86 to 65 degrees was reported. The oxygen content of the sample surface increased to 20%, which resulted in a change of the O/C ratio from 0.149 to 0.265. This increase is greater than what was achieved in our study, but it should be considered that we employed low power and exposure duration. It should also be noted that the authors reported the presence of Cl on the surface of the material [61]. Similarly to the previously mentioned studies, the treatment in the air caused an increase of oxygen from 11 to 22% in the study reported by [59]. Furthermore, the chlorine (Cl 1 s) content dropped from 18 to 10% due to the plasma treatment compared with the reference one. Asadinezhad et al. [62] and Miao et al. [63] also showed that plasma treatment of PVC induces etching and an ablation process, which leads to dehydrochlorination and the introduction of oxygen-containing groups.

Table 5
Atomic percentage of elements on the surface of the PVC sample.

at %	C 1s	O 1s	Cl 2p	Ca 2p	Si 2p	O/C
Reference	87.58	10.32	0.80	0.48	0.82	0.12
Plasma 2 W, 8 s	81.88	13.45	0.94	2.89	0.84	0.16
Plasma 7 W, 8 s	78.87	17.18	0.83	2.37	0.75	0.22

Table 6
The components of high-resolution C 1 s spectra and their percentage contributions.

FWHM 1.1 ± 0.05, eV	C-C/ C—H	C—CHCl	C–O/ C–OH	C-Cl	C═O/ O–C–O	O–C═O/ COOH
BE, eV	285.0	285.9	286.6	287.0	288.0	289.2
Reference	83.5	8.2	0.1	3.6	0.4	4.2
Plasma 2 W, 8 s	74.9	7.8	3.1	5.7	2.2	5.3
Plasma 7 W, 8 s	72.4	7.2	3.5	6.1	2.7	8.1

Chemical changes measured with XPS correlate with the corresponding WCA results, suggesting that surface oxidation, involving the introduction of oxygen-containing polar groups after plasma treatments, is the primary reason for the surface change. Our results are comparable to the results previously reported, while the treatment time of the materials is in the order of seconds. Also, the results presented above highlight the dual functionality of SDBD as both an activation tool and a surface "cleaning" agent that removes loose additives.

3.5. HPLC/MS analysis

In alignment with the March 2026 European "Safe-and-Sustainable-by-Design" (SSbD) framework [64], the HPLC/MS analysis was conducted to identify substances that may have been released into the treated liquids during and after the plasma treatment of the polymer tubes.

3.5.1. PTFE samples analysis

The intense defluorination of PTFE observed in XPS must result in the release of fluorinated fragments into the process environment. The set of PTFE samples was prepared by igniting the plasma ring in the same location for a duration ranging from 10 s to 5 min, at an applied power of 1–15 W. When the treatment time was extended, and the discharge power increased to 15 W, a pinhole effect (local damage) occurred, causing burning of the material and damage to the tube. MS analysis of the liquid involved revealed peaks corresponding to m/z 163 (RT = 3.87), m/z 263 (RT = 10.58), m/z 313 (RT = 12.85), m/z 363 (RT = 14.53), and m/z 413 (RT = 15.88), which are associated with perfluoropropanoic acid (PFPrA), perfluorobutanoic acid (PFBA), perfluoropentanoic acid (PFPeA), perfluorohexanoic acid (PFHxA), perfluoroheptanoic acid (PFHpA), and perfluorooctanoic acid (PFOA). These compounds belong to the class of perfluorocarboxylic acids, with a molecular formula corresponding to $C_nF_{2n+1}COO^-$, where n ranges from 2 to 7. However, by reducing the plasma exposure time and the discharge power suitable for material processing, the concentrations of these acids decreased. Heavier acids were not detected (Table 7).

The leaching of these species into the liquid over time post-plasma treatment was also investigated. Crucially, our leaching tests showed that these compounds were not detected in the distilled water samples collected at 4, 24, 48, 72, or 96 h post-treatment. This leads to the conclusion that PFAS release is strictly a process-related byproduct of the discharge-driven etching and is not a long-term leaching risk for the final product. However, this identifies a critical industrial need for the integration of downstream water purification (e.g., active carbon filtration or secondary plasma destruction) to ensure "zero-emission" plasma manufacturing.

3.5.2. PVC samples analysis

In contrast to the stable post-treatment behavior of PTFE, PVC tubes exhibited continuous leaching of additives. The results of the PVC tube leaching tests are summarized in Tables 8 and 9. No leaching of DEHP was observed in the reference samples for up to 96 h of storage.

Table 7
The concentration of by-products after plasma treatment of the PTFE tube surface.

Conditions	Molecule	*m/z*	Concentration, M
Reference	PFHxA	313	$<1.0{\cdot}10^{-8}$
	PFPeA	263	$<1.0{\cdot}10^{-8}$
	PFBA	213	$<3.0{\cdot}10^{-8}$
	PFPrA	163	$<3.0{\cdot}10^{-8}$
Plasma 2 W, 4 s	PFHxA	313	$<1.0{\cdot}10^{-8}$
	PFPeA	263	$2.12{\cdot}10^{-8}$
	PFBA	213	$3.70{\cdot}10^{-8}$
	PFPrA	163	$4.64{\cdot}10^{-8}$
Plasma 2 W, 8 s	PFHxA	313	$4.02{\cdot}10^{-8}$
	PFPeA	263	$6.98{\cdot}10^{-8}$
	PFBA	213	$1.39{\cdot}10^{-7}$
	PFPrA	163	$1.77{\cdot}10^{-7}$
Plasma 7 W, 4 s	PFHxA	313	$3.52{\cdot}10^{-8}$
	PFPeA	263	$5.99{\cdot}10^{-8}$
	PFBA	213	$1.31{\cdot}10^{-7}$
	PFPrA	163	$1.45{\cdot}10^{-7}$
Plasma 7 W, 8 s	PFHxA	313	$5.17{\cdot}10^{-8}$
	PFPeA	263	$9.68{\cdot}10^{-8}$
	PFBA	213	$2.11{\cdot}10^{-7}$
	PFPrA	163	$2.76{\cdot}10^{-7}$

However, low concentrations of phthalic acid were identified after 72 and 96 h, indicating gradual accumulation over time. This behavior is most likely attributed to the slow hydrolysis and/or oxidative degradation of residual plasticizer molecules inherently present in the PVC matrix. As DEHP is not chemically bound to the polymer, its gradual transformation into lower molecular weight compounds such as phthalic acid can occur even under mild conditions. Additionally, trace amounts of phthalic acid or partially degraded plasticizer may already be present in the material as a result of its manufacturing or storage history.

Following the plasma treatment, both phthalic acid and DEHP were detected in the leachates. Immediately after treatment (T_0), the concentrations of phthalic acid reached 9.53×10^{-7} M and 1.15×10^{-6} M for discharge powers of 2 and 7 W, respectively. Corresponding DEHP concentrations were 3.21×10^{-7} M and 4.31×10^{-7} M. Although the differences between the two applied powers are relatively small, the temporal evolution of the leaching profiles indicates that higher plasma power accelerates the initial release of phthalic acid into the solution. In contrast, DEHP concentrations remained below the detection limit until 48 h post treatment, after which they increased progressively, reaching levels comparable to those of phthalic acid.

The presence of phthalic acid in the leaching experiments, despite the use of fresh water, indicates that its origin is primarily associated with the material itself rather than with in situ reactions in the liquid phase. Plasma treatment modifies the near-surface region of the polymer, leading to the partial degradation of DEHP and the formation of more polar oxidation products such as phthalic acid. In addition, trace amounts of phthalic acid may already be present in the commercial PVC as residual impurities or as products of prior aging and processing. These species, whether pre-existing or newly formed during plasma exposure, are likely concentrated within the surface layer and are subsequently released upon immersion. In contrast, DEHP, due to its hydrophobic nature and predominant localization in the polymer bulk, diffuses more slowly and becomes detectable only after extended leaching times. The higher concentration of phthalic acid compared to DEHP can therefore be attributed to its preferential presence and formation in the near-surface region, combined with its significantly greater solubility in the aqueous phase.

Rose et al. associated an increasing incubation temperature with significantly increased DEHP levels [65]. Bis(2-ethylhexyl) phthalate has limited solubility in aqueous solutions (approximately 3 ng/ml) in distilled water at 20 °C, but is non-covalently bound to PVC, so it will leach into an aqueous solution at higher temperatures and during the mechanical stress associated with dynamic flow.

To distinguish the influence of plasma discharge on the tube surface from the thermal leaching effect, a critical control experiment was performed. The PVC tube was heated by the heat gun to approximately 50 ± 5 °C, and then washed with distilled water, which was subsequently analyzed. The analysis revealed no phthalic acid in the water, but the DEHP concentration was $1.53{\cdot}10^{-6}$ M, the highest recorded during the measurements. This observation indicates that temperature is the dominant factor governing DEHP migration from the polymer bulk, promoting its diffusion into the aqueous phase without inducing significant chemical transformation. This behavior is consistent with the proposed mechanism, where DEHP is primarily stored within the bulk of the material and released under conditions that enhance molecular mobility. In contrast, phthalic acid is associated mainly with the near-surface region, originating either from pre-existing traces in the material or from plasma-induced degradation of DEHP during treatment. Consequently, its presence in leaching experiments is linked to surface-related processes, whereas DEHP release is controlled by diffusion-driven mechanisms that are strongly temperature-dependent.

When the tubes are processed with SDBD, the polymer's temperature is affected by various factors, including the tube thickness, the applied power, the treatment duration, and the conductivity of the solution used. Adjusting these parameters can help to optimize the temperature load on the treated polymer.

Extensive research on the DEHP leaching effect from a narrow PVC tube was previously done [65–68]. However, only a few studies investigated the effect of plasma treatment on plasticizer leaching. One of the reasons is the impossibility of treating long medical tubes with plasma discharges. Reducing the length of the tube results in very low concentrations that are on the edge of the limit of quantification, as in the case of this study.

For example, in [69] a DC glow discharge plasma generated in Ar

Table 8
Phthalic acid concentration, M.

Conditions	Time 0	4 h	24 h	48 h	72 h	96 h
Reference	$<2.0{\cdot}10^{-7}$	$<2.0{\cdot}10^{-7}$	$<2.0{\cdot}10^{-7}$	$<2.0{\cdot}10^{-7}$	$3.52{\cdot}10^{-7}$	$5.02{\cdot}10^{-7}$
Heated	-					
Plasma 2 W, 8 s	$9.53{\cdot}10^{-7}$	$<2.0{\cdot}10^{-7}$	$2.07{\cdot}10^{-7}$	$4.20{\cdot}10^{-7}$	$8.99{\cdot}10^{-7}$	$1.45{\cdot}10^{-6}$
Plasma 7 W, 8 s	$1.15{\cdot}10^{-6}$	$3.13{\cdot}10^{-7}$	$4.91{\cdot}10^{-7}$	$7.46{\cdot}10^{-7}$	$9.00{\cdot}10^{-7}$	$1.51{\cdot}10^{-6}$

Table 9
DEHP concentration, M.

Conditions	Time 0	4 h	24 hours	48 h	72 h	96 h
Reference	$<2.0{\cdot}10^{-7}$	$<2.0{\cdot}10^{-7}$	$<2.0{\cdot}10^{-7}$	$<2.0{\cdot}10^{-7}$	$<2.0{\cdot}10^{-7}$	$<2.0{\cdot}10^{-7}$
Heated	$1.53{\cdot}10^{-6}$					
Plasma 2 W, 8 s	$3.21{\cdot}10^{-7}$	$<2.0{\cdot}10^{-7}$	$<2.0{\cdot}10^{-7}$	$<2.0{\cdot}10^{-7}$	$7.49{\cdot}10^{-7}$	$1.04{\cdot}10^{-6}$
Plasma 7 W, 8 s	$4.31{\cdot}10^{-7}$	$<2.0{\cdot}10^{-7}$	$<2.0{\cdot}10^{-7}$	$<2.0{\cdot}10^{-7}$	$8.17{\cdot}10^{-7}$	$1.00{\cdot}10^{-6}$

inside the tube was investigated. The amount of plasticizer leached from the inner surface of the PVC tubes was measured. It was found that the applied voltage had little effect on the leaching of the plasticizer and that the amount of leached plasticizer decreased with increasing treatment time and decreasing pressure. The maximum amount of extracted plasticizer was reported to be approximately 300 μg/mL. This value is almost twice as high as our results reported here.

As discussed previously, the formation and release of phthalic acid can be attributed to the plasma-induced degradation of DEHP during tube plasma treatment. For example, [70] reported phthalic acid as a degradation product of dimethyl phthalate treated in a microplasma system designed for the degradation of water contaminants. Moreover, they observed an almost complete conversion of dimethyl phthalate into CO, CO_2, and H_2O and attributed this high degree of mineralization to the efficient generation of OH radicals and ozone in their system. The analyses of RONS in the liquid that was in contact with plasma in our configuration proved the presence of hydrogen peroxide in considerable amounts, supporting the suggested assumption [18].

While plasma treatment clearly improves the surface properties of polymeric tubes, a potential concern arises regarding the release of DEHP and its degradation products, such as phthalic acid, during post-treatment washing or handling. To address this, an additional plasma treatment stage could be integrated at the end of the production line to degrade any residual phthalates directly in the process water. Previous studies have reported efficient plasma degradation of phthalates using various gases [71,72] and liquid phase plasma discharges [73] in soil and water matrices. Furthermore, to enhance the energy efficiency of phthalate degradation using plasma treatment, the synergistic effect of various catalysts and added chemicals has also been proven in hybrid plasma plus catalyst reactors [73,74]

Overall, the present study demonstrates that plasma treatment is a versatile approach to polymeric tubing functionalization, enabling not only effective surface activation and cleaning but also partial degradation of embedded additives such as DEHP. This dual functionality makes plasma technology particularly attractive for applications that demand both high material performance and improved safety standards. As we move toward 2030, the integration of these environmental safety metrics will become the standard for all plasma-assisted manufacturing processes.

At the same time, the findings emphasize an important consideration: although plasma can break down surface-bound plasticizers, some by-products may remain mobile and be released later. Therefore, coupling the plasma modification step with a downstream plasma-based purification process offers a practical strategy to eliminate residual contaminants, ultimately supporting the production of safer and more sustainable polymeric materials.

4. Conclusions

This study demonstrates that non-thermal plasma generated via a liquid-electrode surface dielectric barrier discharge effectively overcomes the geometric limitations of conventional planar systems, enabling uniform internal surface modification of narrow polymer tubes without compromising material bulk integrity. Water contact angle measurements confirmed a successful shift to hydrophilic states (WCA ≈ 65–75°) for both PTFE and PVC, which was supported by spectroscopic analyses showing enhanced oxygen-containing functional groups and a modest increase in surface roughness that can improve adhesion properties.

Crucially, an integrated environmental safety assessment using HPLC/MS revealed distinct leaching behaviors between the two materials upon sDBD treatment with liquid electrode. In PTFE, trace concentrations of by-products were detectable only immediately after treatment, suggesting that the fluoropolymer inherent chemical stability limited further degradation over time. In contrast, the PVC analysis highlighted a critical distinction between thermal and plasma-chemical effects: while di(2-ethylhexyl) phthalate leaching was confirmed to be a temperature-driven diffusion process, the formation of phthalic acid emerged as a unique signature of plasma-induced oxidative degradation. While these findings highlight a critical dual effect, where the plasma mechanisms driving surface functionalization also contribute to minor structural disruption and additive migration, they underscore the necessity of balancing surface performance with regulatory compliance. Ultimately, refining plasma parameters and employing strategies such as post-treatment stabilization will be essential for safely harnessing plasma technology in sensitive medical and industrial applications.

Funding

This work was funded by the EU NextGenerationEU through the Recovery and Resilience Plan for Slovakia under the project No 09I03-03-V04-00094 and by the project LM2023039 funded by the Ministry of Education, Youth and Sports of the Czech Republic.

CRediT authorship contribution statement

Oleksandr Galmiz: Writing – review & editing, Writing – original draft, Project administration, Methodology, Investigation, Funding acquisition, Formal analysis, Data curation, Conceptualization. **Giulia Tomei:** Writing – review & editing, Investigation, Formal analysis, Data curation. **Ester Marotta:** Writing – review & editing, Supervision. **Zdenko Machala:** Writing – review & editing, Supervision, Project administration.

Declaration of competing interest

The authors declare that they have no known competing financial interests or personal relationships that could have appeared to influence the work reported in this paper.

Data availability

Data will be made available on request.

References

[1] K.D Weltmann, T. Von Woedtke, Plasma medicine - current state of research and medical application, Plasma Phys. Control. Fusion 59 (2017) 014031, https://doi.org/10.1088/0741-3335/59/1/014031.
[2] Y. Xu, A. Bassi, Non-thermal plasma decontamination of microbes: a state of the art, Biotechnol. Prog. 41 (2025) e3511, https://doi.org/10.1002/btpr.3511.
[3] S. Sammut, A comprehensive review of plasma cleaning processes used in semiconductor packaging, Appl. Sci. 15 (15) (2025) 7361, https://doi.org/10.3390/app15137361.
[4] N. Puač, N. Škoro, Plasma–Liquid interaction for agriculture—a focused review, Plasma Process. Polym. 22 (2025) 2400208, https://doi.org/10.1002/ppap.202400208.
[5] M. Fleischer, Z. Kelar Tučeková, O. Galmiz, et al., Plasma treatment of large-area polymer substrates for the enhanced adhesion of UV–digital printing, Nanomaterials 14 (5) (2024) 426, https://doi.org/10.3390/nano14050426.
[6] L. Janů, E. Dvořáková, K. Polášková, et al., Enhanced adhesion of electrospun polycaprolactone nanofibers to plasma-modified polypropylene fabric, Polymers 15 (7) (2023) 1686, https://doi.org/10.3390/polym15071686.
[7] J.P Booth, M. Mozetič, A. Nikiforov, C. Oehr, Foundations of plasma surface functionalization of polymers for industrial and biological applications, Plasma Sources. Sci. Technol. 31 (2022) 103001, https://doi.org/10.1088/1361-6595/ac70f9.
[8] C. Ma, A. Nikiforov, D. Hegemann, et al., Plasma-controlled surface wettability: recent advances and future applications, Int. Mater. Rev. 68 (2023) 82–119, https://doi.org/10.1080/09506608.2022.2047420.
[9] S. Kitazaki, N. Hayashi, Sterilization characteristics of tube inner surface using oxygen plasma produced by AC HV discharge, IEEE Trans. Plasma Sci. 36 (2008) 1304–1305, https://doi.org/10.1109/TPS.2008.922451.
[10] C.M Wen, C.H Lin, Tube-based DBD plasma treatment for improving the performance of the slippery coating layers on medical catheters, IEEE Trans. Plasma Sci. 49 (2021) 162–167, https://doi.org/10.1109/TPS.2020.3009409.
[11] S. Wu, Y. Guo, F. Ouyang, et al., Characteristics of the plasma sheath in helium discharge within dielectric tubes, Plasma Sci. Technol. 25 (2023) 045402, https://doi.org/10.1088/2058-6272/ac9e93.

[12] R. Muto, N. Hayashi, Sterilization characteristics of narrow tubing by nitrogen oxides generated in atmospheric pressure air plasma, Sci. Rep. 13 (2023) 6947, https://doi.org/10.1038/s41598-023-34243-3.
[13] N. Hayashi, W. Guan, S. Tsutsui, et al., Sterilization of medical equipment using radicals produced by oxygen/water vapor RF plasma, Jpn. J. Appl. Phys. 45 (2006) 8358–8363, https://doi.org/10.1143/JJAP.45.8358/XML.
[14] R. Prat, Y.J Koh, Y. Babukutty, et al., Polymer deposition using atmospheric pressure plasma glow (APG) discharge, Polym. (Guildf) 41 (2000) 7355–7360, https://doi.org/10.1016/S0032-3861(00)00103-8.
[15] M. Polak, J. Winter, U. Schnabel, et al., Innovative plasma generation in flexible biopsy channels for inner-tube decontamination and medical applications, Plasma Process. Polym. 9 (2012) 67–76, https://doi.org/10.1002/PPAP.201000163;PAGE:STRING:ARTICLE/CHAPTER.
[16] D. Pavliňák, O. Galmiz, M. Zemánek, et al., Permanent hydrophilization of outer and inner surfaces of polytetrafluoroethylene tubes using ambient air plasma generated by surface dielectric barrier discharges, Appl. Phys. Lett. 105 (2014) 154102, https://doi.org/10.1063/1.4898134.
[17] O. Galmiz, R. Cimerman, P. Pareek, et al., Production of reactive species by using surface dielectric barrier discharge in direct contact with water, Plasma Sources. Sci. Technol. 34 (2025) 025011, https://doi.org/10.1088/1361-6595/adb3cb.
[18] O. Galmiz, R. Cimerman, Z. Machala, Effect of reactor configuration of surface dielectric barrier discharge in contact with liquids on the production of reactive species, Chem. Eng. J. 530 (2026) 173630, https://doi.org/10.1016/j.cej.2026.173630.
[19] A. Khlyustova, O. Galmiz, M. Zahoran, Underwater discharge plasma-induced coating of poly(acrylic acid) on polypropylene fiber, J. Mater. Sci. 50 (2015) 3504–3509, https://doi.org/10.1007/s10853-015-8913-4.
[20] O. Galmiz, D. Pavlinak, M. Zemanek, et al., Study of surface dielectric barrier discharge generated using liquid electrodes in different gases, J. Phys. D. Appl. Phys. 49 (2016) 065201, https://doi.org/10.1088/0022-3727/49/6/065201.
[21] M. Darmanin, A. Fröhling, S. Bußler, et al., Aqueous and gaseous plasma applications for the treatment of mung bean seeds, Sci. Rep. 11 (1) (2021) 19681, https://doi.org/10.1038/s41598-021-97823-1.
[22] P.R Rotondo, D. Aceto, M. Ambrico, et al., Physicochemical properties of plasma-activated water and associated antimicrobial activity against fungi and bacteria, Sci. Rep. 15 (1) (2025) 5536, https://doi.org/10.1038/s41598-025-88369-7.
[23] G. Primc, Recent advances in surface activation of polytetrafluoroethylene (PTFE) by gaseous plasma treatments, Polymers 12 (2020) 2295, https://doi.org/10.3390/POLYM12102295.
[24] S. Jamali, A. Kargarian, Comparative study of surface modification of fluorinated and non-fluorinated polymers using SDBD air plasma, Sci. Rep. 15 (2025) 35917, https://doi.org/10.1038/s41598-025-19841-7.
[25] J.L Sims, K.M Stroski, S. Kim, et al., Global occurrence and probabilistic environmental health hazard assessment of per- and polyfluoroalkyl substances (PFASs) in groundwater and surface waters, Sci. Total Environ. 816 (2022) 151535, https://doi.org/10.1016/j.scitotenv.2021.151535.
[26] M. Antonopoulou, A. Spyrou, A. Tzamaria, et al., Current state of knowledge of environmental occurrence, toxic effects, and advanced treatment of PFOS and PFOA, Sci. Total Environ. 913 (2024) 169332, https://doi.org/10.1016/j.scitotenv.2023.169332.
[27] M. Hamza, R.T Ayinla, I. Elsayed, E.B Hassan, Understanding PFAS adsorption: how molecular structure affects sustainable water treatment, Environments 12 (2025) 330, https://doi.org/10.3390/environments12090330.
[28] K. Houssini, J. Li, Q. Tan, Complexities of the global plastics supply chain revealed in a trade-linked material flow analysis, Commun. Earth Environ. 6 (1) (2025) 257, https://doi.org/10.1038/s43247-025-02169-5.
[29] G. Latini, M. Ferri, F. Chiellini, Materials degradation in PVC medical devices, DEHP leaching and neonatal outcomes, Curr. Med. Chem. 17 (2010) 2979–2989.
[30] IARC (International Agency for Research on Cancer), Some Chemicals Present in Industrial and Consumer products, Food and Drinking-Water, IARC Monogr Eval Carcinog Risks Hum, 2012, pp. 149–284.
[31] X. Zhang, C. Zhang, J.M Hankett, Z. Chen, Molecular surface structural changes of plasticized PVC materials after plasma treatment, Langmuir 29 (2013) 4008–4018, https://doi.org/10.1021/la4000796.
[32] J.L Fugit, J.L Taverdet, J.Y Gauvrit, P. Lanteri, Treatment of plasticized PVC to reduce plasticizer/solvent migration: optimization with an experimental design, Polym. Int. 52 (2003) 670–675, https://doi.org/10.1002/PI.971.
[33] M.T Khorasani, H. Mirzadeh, Effect of oxygen plasma treatment on surface charge and wettability of PVC blood bag - In vitro assay, Radiat. Phys. Chem. 76 (2007) 1011–1016, https://doi.org/10.1016/j.radphyschem.2006.10.002.
[34] A.R Hoskinson, N. Hershkowitz, Differences between dielectric barrier discharge plasma actuators with cylindrical and rectangular exposed electrodes, J. Phys. D. Appl. Phys. 43 (2010) 065205, https://doi.org/10.1088/0022-3727/43/6/065205.
[35] E. Moreau, C. Louste, G. Touchard, Electric wind induced by sliding discharge in air at atmospheric pressure, J. Electrostat. 66 (2008) 107–114, https://doi.org/10.1016/j.elstat.2007.08.011.
[36] H. Grosch, T. Hoder, K.D Weltmann, R. Brandenburg, Spatio-temporal development of microdischarges in a surface barrier discharge arrangement in air at atmospheric pressure, Eur. Phys. J. D 60 (2010) 547–553, https://doi.org/10.1140/epjd/e2010-00239-8.
[37] K. Allegraud, O. Guaitella, A. Rousseau, Spatio-temporal breakdown in surface DBDs: evidence of collective effect, J. Phys. D. Appl. Phys. 40 (2007) 7698–7706, https://doi.org/10.1088/0022-3727/40/24/017.
[38] O. Galmiz, D. Pavlinak, M. Zemanek, et al., Study of surface dielectric barrier discharge generated using liquid electrodes in different gases, J. Phys. D. Appl. Phys. 49 (2016) 065201, https://doi.org/10.1088/0022-3727/49/6/065201.
[39] N.M Jordan, Y.Y Lau, D.M French, et al., Electric field and electron orbits near a triple point, J. Appl. Phys. 102 (2007) 033301, https://doi.org/10.1063/1.2764211.
[40] R. Brandenburg, Dielectric barrier discharges: progress on plasma sources and on the understanding of regimes and single filaments, Plasma Sources Sci. Technol. 26 (2017) 053001, https://doi.org/10.1088/1361-6595/AA6426.
[41] N. Cvetanović, O. Galmiz, P. Synek, et al., Electron density in surface barrier discharge emerging at argon/water interface: quantification for streamers and leaders, Plasma Sources Sci. Technol. 27 (2018) 025002, https://doi.org/10.1088/1361-6595/aaa578.
[42] J. Voráč, P. Synek, V. Procházka, T. Hoder, State-by-state emission spectra fitting for non-equilibrium plasmas: OH spectra of surface barrier discharge at argon/water interface, J. Phys. D. Appl. Phys. 50 (2017) 294002, https://doi.org/10.1088/1361-6463/aa7570.
[43] O. Galmiz, D. Pavliňák, M. Zemánek, et al., Hydrophilization of outer and inner surfaces of Poly(vinyl chloride) tubes using surface dielectric barrier discharges generated in ambient air plasma, Plasma Process. Polym. 14 (2017) e1600220, https://doi.org/10.1002/ppap.201600220.
[44] C. Liu, N. Cui, N.M.D Brown, B.J Meenan, Effects of DBD plasma operating parameters on the polymer surface modification, Surf. Coat. Technol. 185 (2004) 311–320, https://doi.org/10.1016/J.SURFCOAT.2004.01.024.
[45] Z. Fang, Y. Qiu, Y. Luo, Surface modification of polytetrafluoroethylene film using the atmospheric pressure glow discharge in air, J. Phys. D. Appl. Phys. 36 (2003) 2980–2985, https://doi.org/10.1088/0022-3727/36/23/019.
[46] M. Ghoranneviss, S. Shahidi, J. Wiener, Surface modification of poly vinyl chloride (PVC) using low pressure argon and oxygen plasma, Plasma Sci. Technol. 12 (2010) 204–207, https://doi.org/10.1088/1009-0630/12/2/14.
[47] I. Banik, K.S Kim, Y.I Yun, et al., A closer look into the behavior of oxygen plasma-treated high-density polyethylene, Polymer 44 (2003) 1163–1170, https://doi.org/10.1016/S0032-3861(02)00847-9.
[48] J. Larrieu, B. Held, H. Martinez, Y. Tison, Ageing of atactic and isotactic polystyrene thin films treated by oxygen DC pulsed plasma, Surf. Coat. Technol. 200 (2005) 2310–2316, https://doi.org/10.1016/j.surfcoat.2004.06.032.
[49] R. Morent, N. De Geyter, C. Leys, et al., Study of the ageing behaviour of polymer films treated with a dielectric barrier discharge in air, helium and argon at medium pressure, Surf. Coat. Technol. 201 (2007) 7847–7854, https://doi.org/10.1016/j.surfcoat.2007.03.018.
[50] M. Okubo, Nonthermal plasma surface modification of fluoropolymer plastic films: a review (invited paper), J. Electrostat. 137 (2025) 104114, https://doi.org/10.1016/J.ELSTAT.2025.104114.
[51] J. Ren, J. Li, Y. Zhen, et al., Removal of polyvinyl chloride microplastic by dielectric barrier discharge plasma, Sep. Purif. Technol. 290 (2022) 120832, https://doi.org/10.1016/J.SEPPUR.2022.120832.
[52] M.F Bekkara, L. Dascalescu, Y. Benmimoun, et al., Modification of surface characteristic and tribo-electric properties of polymers by DBD plasma in atmospheric air, Eur. Phys. J. Appl. Phys. 81 (2018) 10801, https://doi.org/10.1051/EPJAP/2017170149.
[53] A. Asadinezhad, M. Lehocký, P. Sáha, M. Mozetič, Recent progress in surface modification of polyvinyl chloride, Materials 5 (2012) 2937–2959, https://doi.org/10.3390/MA5122937.
[54] Q.N Xu, H.L Wang, J.P Liang, et al., Atmospheric air and liquid-film DBD plasma using sine AC excitations for purpose of improving the hydrophilicity of PTFE, Vacuum 207 (2023) 111688, https://doi.org/10.1016/J.VACUUM.2022.111688.
[55] C. Sarra-Bournet, S. Turgeon, D. Mantovani, G. Laroche, A study of atmospheric pressure plasma discharges for surface functionalization of PTFE used in biomedical applications, J. Phys. D. Appl. Phys. 39 (2006) 3461–3469, https://doi.org/10.1088/0022-3727/39/16/S03.
[56] M. Chen, P.O Zamora, P. Som, et al., Cell attachment and biocompatibility of polytetrafluoroethylene (PTFE) treated with glow-discharge plasma of mixed ammonia and oxygen, J. Biomater. Sci. Polym. Ed. 14 (2003) 917–935, https://doi.org/10.1163/156856203322381410.
[57] N. Vandencasteele, H. Fairbrother, F. Reniers, Selected effect of the ions and the neutrals in the plasma treatment of PTFE surfaces: an OES-AFM-contact angle and XPS study, Plasma Process. Polym. 2 (2005) 493–500, https://doi.org/10.1002/PPAP.200500010.
[58] D. Wilson, A. Eccles, T. Steele, et al., Surface chemistry and wettability of plasma-treated PTFE, Surf. Interface Anal. 30 (2000) 36–39.
[59] A. Suganya, G. Shanmugavelayutham, C.S Rodríguez, Study on structural, morphological and thermal properties of surface modified polyvinylchloride (PVC) film under air, argon and oxygen discharge plasma, Mater. Res. Express. 3 (2016) 095302, https://doi.org/10.1088/2053-1591/3/9/095302.
[60] D.J Balazs, K. Triandafillu, P. Wood, et al., Inhibition of bacterial adhesion on PVC endotracheal tubes by RF-oxygen glow discharge, sodium hydroxide and silver nitrate treatments, Biomaterials 25 (2004) 2139–2151, https://doi.org/10.1016/j.biomaterials.2003.08.053.
[61] A. Asadinezhad, I. Novak, M. Lehocky, et al., A physicochemical approach to render antibacterial surfaces on plasma-treated medical-grade PVC: irgasan coating, Plasma Process. Polym. 7 (2010) 504–514, https://doi.org/10.1002/ppap.200900132.
[62] A. Asadinezhad, I. Novák, M. Lehocký, et al., An in vitro bacterial adhesion assessment of surface-modified medical-grade PVC, Colloids Surf. B Biointerfaces 77 (2010) 246–256, https://doi.org/10.1016/J.COLSURFB.2010.02.006.

[63] H. Miao, C. Jierong, Inactivation of *Escherichia coli* and properties of medical poly (vinyl chloride) in remote-oxygen plasma, Appl. Surf. Sci. 255 (2009) 5690–5697, https://doi.org/10.1016/J.APSUSC.2008.12.056.
[64] Safe and sustainable by design - research and innovation. https://research-and-innovation.ec.europa.eu/research-area/industrial-research-and-innovation/chemicals-and-advanced-materials/safe-and-sustainable-design_en. Accessed 20 Mar 2026.
[65] R.J Rose, M.J Priston, A.E Rigby-Jones, J.R Sneyd, The effect of temperature on di (2-ethylhexyl) phthalate leaching from PVC infusion sets exposed to lipid emulsions, Anaesthesia 67 (2012) 514–520, https://doi.org/10.1111/J.1365-2044.2011.07006.X.
[66] S. Loff, F. Kabs, U. Subotic, et al., Kinetics of diethylhexyl-phthalate extraction from polyvinylchloride-infusion lines, J. Parenter. Enter. Nutr. 26 (2002) 305–309, https://doi.org/10.1177/0148607102026005305.
[67] S. Takatori, Y. Okamoto, Y. Kitagawa, et al., Simulated neonatal exposure to DEHP and MEHP from PVC enteral nutrition products, Int. J. Pharm. 352 (2008) 139–145, https://doi.org/10.1016/J.IJPHARM.2007.10.020.
[68] H. Takehisa, E. Naoko, S. Masahiko, et al., Release behavior of diethylhexyl phthalate from the polyvinyl-chloride tubing used for intravenous administration and the plasticized PVC membrane, Int. J. Pharm. 297 (2005) 30–37, https://doi.org/10.1016/J.IJPHARM.2005.02.015.
[69] X.Q Wen, X.H Liu, G.S Liu, Prevention of plasticizer leaching from the inner surface of narrow polyvinyl chloride tube by DC glow discharge plasma, IEEE Trans. Plasma Sci. 38 (2010) 3152–3155, https://doi.org/10.1109/TPS.2010.2074209.
[70] Z.H Qi, L. Yang, Y. Xia, et al., Removal of dimethyl phthalate in water by non-thermal air plasma treatment, Env. Sci (Camb.) 5 (2019) 920–930, https://doi.org/10.1039/C9EW00072K.
[71] H. Kan, T. Wang, Z. Yang, et al., High frequency discharge plasma induced plasticizer elimination in water: removal performance and residual toxicity, J. Hazard. Mater. 383 (2020) 121185, https://doi.org/10.1016/J.JHAZMAT.2019.121185.
[72] K. Ulucan-Altuntas, M. Saleem, G. Tomei, et al., Atmospheric plasma-based approaches for the degradation of dimethyl phthalate (DMP) in water, J. Env. Manage. 301 (2022) 113885, https://doi.org/10.1016/J.JENVMAN.2021.113885.
[73] H. Lee, Y.K Park, J.S Kim, et al., Degradation of dimethyl phthalate using a liquid phase plasma process with TiO2 photocatalysts, Env. Res. 169 (2019) 256–260, https://doi.org/10.1016/J.ENVRES.2018.11.025.
[74] E. Ahmadi, B. Shokri, A. Mesdaghinia, et al., Synergistic effects of α-Fe2O3-TiO2 and Na2S2O8 on the performance of a non-thermal plasma reactor as a novel catalytic oxidation process for dimethyl phthalate degradation, Sep. Purif. Technol. 250 (2020) 117185, https://doi.org/10.1016/J.SEPPUR.2020.117185.